

# EXPERIMENTAL INVESTIGATION OF SURFACE ROUGHNESS OF CT3 STEEL ON ADHESION STRENGTH OF ARC SPRAY Al-Mg ALLOY COATING

Le Duc Thanh<sup>1</sup>, Nguyen Thi Hai Van<sup>2\*</sup>, Ha Pham Thi<sup>3</sup>, Trinh Quang Hung<sup>1</sup>

<sup>1</sup>Le Quy Don Technical University, Hanoi, Vietnam

<sup>2</sup>The University of Danang - University of Technology and Education, Danang, Vietnam

<sup>3</sup>Institute for Tropical Technology, Vietnam Academy of Science and Technology, Hanoi, Vietnam

\*Corresponding author: nthvan@ute.udn.vn

(Received: July 25, 2023; Revised: September 20, 2023; Accepted: October 26, 2023)

**Abstract** - Thermal spray-applied AlMg alloy coatings are frequently utilized in a variety of technical applications because of great corrosion resistance, and environmental friendliness. In this work, the effect of abrasive spraying parameters on the surface roughness of CT3 steel specimens as well as the effect of the surface roughness on the adhesion strength of Al-Mg alloy spray coating were experimentally investigated. The surface roughness was assessed using a portable roughness gauge. The adhesion strength of the coating was evaluated by the pull-off test, according to the JIS H8664-1977 standard. The experimental findings indicate that air pressure and spraying distance have great impacts on the surface roughness of CT3 steel. The adhesion strength of the Al-Mg coating applied on CT3 steel is found to be almost linearly proportional to the surface roughness. The maximum adhesion strength of 14 MPa was achieved at the highest Rz of about 61  $\mu\text{m}$ .

**Key words** - Spray coating; surface roughness; regression; Taguchi experimental planning approach

## 1. Introduction

Since maritime buildings and equipment inevitably corrode over time, corrosion in the marine environment is a growing worry for nations all over the world. According to research findings from 2014, corrosion-related losses in China totaled roughly 3.34% of GDP, but more than a third of that loss was attributable to corrosion in the marine environment [1]. One of the best and most popular techniques for preventing corrosion is the application of coatings, especially metal coatings [2-3]. Common methods for metal coating include hot-dip galvanizing and thermal spraying [4-7]. Thermal coating is advised for metal coating applications to give steel substrates with corrosion resistance in most situations [8-12]. AlMg alloy coatings have proven to be reliable and effective at preventing corrosion in marine environments [13-14]. AlMg coatings are frequently utilized in a variety of technical applications because of their low weight, strong mechanical characteristics, great corrosion resistance, and environmental friendliness. AlMg alloy coatings have demonstrated their efficacy and dependability in preventing corrosion in marine conditions. The addition of Mg to the coating boosts Al's ability to actively protect as a sacrificial anode. On the other hand, the AlMg coating has a higher hardness than pure Al, boosting its capacity to function in harsh environments [15].

Substrate surface pre-spray treatment before thermal spraying is one of the most important factors affecting the quality of the thermal spray coating. Proper cleaning and

roughening of the substrate surface provide the best conditions for the contact process of the first molten particles that strike the substrate surface during the thermal spraying process.

According to previous studies, the surface roughness of the substrate has a great influence on the quality of the thermal spray coating, especially the adhesion strength - a very important criterion of the coating [16-19].

In the study [16], Al coating was fabricated on substrates of various roughness and with or without preheating (at 120°C), with different spraying processes, namely flame spraying (FS), high-velocity oxy-fuel (HVOF) spraying and twin-wire arc spraying. Spray mode to roughen the steel surface is as follows: 90° impingement angle, Alundum 38A aluminum oxide abrasive powder, variable stand-off distance of 100, 140, 180 mm, and 100 psi blasting pressure and 60-80s spray time. The surface roughness of the steel substrate is measured at 5 locations on the surface and the average value is taken. The results show that the adhesion of the coatings deposited by HVOF and electric arc spraying on the steel substrate surface with higher roughness, without preheating, reaches the required value according to the standard. Meanwhile, the coating deposited by flame spray has higher adhesion when the steel substrate is preheated. The coating surface roughness decreases as the steel substrate roughness decreases. For machining post-spray coatings with exacting dimensional requirements, it is crucial.

Several researches have shown the influence of substrate surface roughness on the adhesion strength of the copper coatings [17-19]. The copper coating was fabricated by cold spray, which has suitable adhesion on steel substrates when the steel substrate surface is partially polished [17]. However, for a copper coating that was fabricated using cold spray on aluminum substrates, a smoother substrate surface will give a higher adhesion strength [18]. In the study in [19], 316L stainless steel substrates were prepared with different surface roughness using three different methods: hot rolling (without polishing), polishing with 400 grit paper (rough polishing) and polishing with 2000 grit paper (fine polishing). The surface roughness (Ra) of the three above samples is  $5 \pm 1.23 \mu\text{m}$ ,  $0.50 \pm 0.14 \mu\text{m}$  and  $0.06 \pm 0.01 \mu\text{m}$ , respectively. The research showed that the surface roughness of the substrate has an important role in the quality of the coatings. Finely polished substrate surfaces were demonstrated to be better than the hot-rolled and semi-

polished substrate surfaces for achieving better coating quality, such as higher microhardness, and smaller porosity.

Author group Y.-Y. Wang et al. have published research on alloy NiCrBSi and WC-Co coatings fabricated on steel substrates by HVOF with various surface roughness to understand the bonding mechanism of coating and substrate [20]. The results show that when the surface roughness increases, the adhesion of the coating to the base metal also increases. The adhesion mechanism of NiCrBSi coatings to fully molten spray particles is mainly mechanical, while deposition with solid-liquid two-phase spray particles in the WC-Co coating can lead to Van der Waals physical bonds in addition to mechanical bonds.

The influence of parameters in the abrasive blasting process on the surface roughness and coating properties has also been studied [21-25].

The substrate 304L stainless steel was sprayed with Al<sub>2</sub>O<sub>3</sub> abrasive particles at a 45° spray angle, 60 mm injection distance, and variable pneumatic pressure from 2 to 7 bar [21]. The alloy Al<sub>2</sub>O<sub>3</sub> coating was deposited by the air plasma spraying process. The results show that, when the blasting pressure rises, the surface roughness of the steel substrate increases. This results in a decrease in coating hardness, while increasing porosity and coating roughness. The results of this study have not shown the relationship between the surface roughness of the substrate and the adhesion of the coating.

In the study [22], the authors researched the influence of varying the grain size, air pressure, blasting time, blasting angle and stand-off distance on the roughness of the surface of the carbon steel substrate. The experimental results show that the surface roughness was found to increase as the abrasive grain size, compressed air pressure, injection time, or injection angle was increased. The surface residual compressive stress and surface hardness were increased with both blasting pressure and blasting angle.

Alexandra Kemény et al. researched the influence of abrasive blasting modes on the surface roughness of titanium alloy [23]. Five parameters of the abrasive blasting process were investigated, namely abrasive grit size, blasting distance, time of blasting, blasting pressure and blasting angle. Each parameter is tested at three different levels of values. This research used the Taguchi experimental method. The results show that the abrasive grain size has the greatest impact, followed by the pneumatic pressure on the surface roughness. Other parameters have a lower impact on the surface roughness of the substrate.

The effect of abrasive blasting parameters on the surface roughness of aluminum, cast iron and steel alloys has been studied [24]. Variable parameters are stand-off distance, blasting angle and blasting pressure with three sizes of white alumina grit used. The research shows that the abrasive grit size has the greatest influence on the surface roughness of the substrate. The blasting pressure increase leads to slight increases in the roughness. While the blasting time from 3 to 6 seconds is enough to achieve the maximum roughness.

Research on the effect of abrasive blasting angle and

plasma spray angle on the adhesion strength of plasma coatings on titanium alloy substrates has been reported [25]. Five different plasma spray and abrasive blasting angles from 45° to 90° were investigated. The study shows that the maximum adhesion strength is achieved at the plasma spray angle and the abrasive blast angle of 90°.

Thus, with these references, we see that the adhesion strength of the thermal coatings depends on the surface roughness of the substrate, while the surface roughness is greatly influenced by the parameters of the abrasive blasting process. This work aims to experimentally study the influence of process parameters of air pressure and spraying distance on the roughness of CT3 steel samples and the adhesion strength of Al-Mg coatings on the treated substrates. The Taguchi experimental planning approach was applied to explore the dependence of the surface roughness on these parameters and to find the optimum roughing conditions to obtain the highest quality of Al-Mg alloy arc spray coating.

## 2. Materials and experimental methods

### 2.1. Materials

In this study, CT3 steel specimens with dimensions of 50 mm x 50 mm x 3 mm were used as the substrate material and brown corundum Al<sub>2</sub>O<sub>3</sub> (Hai Duong Grinding Joint Stock Company, Vietnam) was used as the abrasive material. The grain size of Al<sub>2</sub>O<sub>3</sub> is G18, which corresponds to about 1.2mm [26].

Al-5Mg alloy wire with a diameter of 2 mm made by Metallisation Ltd (West Midlands, UK) was used as the feedstock for the spray system.

### 2.2. Specimens preparation

Before spraying abrasive particles to create roughness, CT3 steel specimens were processed through several steps, including cutting, grinding, and surface cleaning by soaking the samples in the acetone solvent to remove grease and other impurities. The surfaces of the steel substrates were then wiped dry with a clean cloth.

After being thoroughly cleaned, the steel specimens were subjected to an abrasive spraying process that utilized the brown corundum abrasives. There are numerous aspects, including the nozzle design, air pressure, spraying angle, spraying duration, spraying distance from the nozzle opening to the specimen surface, and abrasive particle size, [27] which all have a role in determining the final roughness. Among them, the air pressure and spraying distance are taken into consideration in this work as the varying modes. The other variables are kept constant during the course of the experiment with their values listed in Table 1.

*Table 1. The fixed abrasive spraying parameters*

Order	Parameter	Value
1	Spraying time	30 seconds
2	Spraying angle	90°
3	Abrasive grit size	mm

In this work, the Taguchi experimental planning method [28] and Minitab statistical analysis software were used to develop a regression mathematical model between

the surface roughness of CT3 steel specimens and the input variables, including the air pressure, and spraying distance. The analysis of variance method (ANOVA) was used to analyze the effect of the aforementioned parameters on the surface roughness of the steel substrate.

The ranges of the parameter values to be tested were determined based on the recommendations and references provided by the equipment providers as follows:

- Blasting pressure,  $P$ : 6 to 8 bar;
- Stand-off distance,  $L$ : 100 to 200 mm.

Table 2 shows the experimental design with two factors and three levels, according to the method proposed by Taguchi.

**Table 2.** Input process parameters

Order	Factor	Values of levels		
		Level 1	Level 2	Level 3
1	$P$ (bar)	6	7	8
2	$L$ (mm)	100	150	200

In the experimental design, each of the input parameters has three distinct levels, and the orthogonal array is L9 (Table 3).

**Table 3.** The orthogonal array L9 of the Taguchi method

Specimens	1	2	3	4	5	6	7	8	9
$P$ (bar)	6	6	6	7	7	7	8	8	8
$L$ (mm)	100	150	200	100	150	200	100	150	200

The experiments were conducted according to Table 3. Each run was repeated three times, and the result for surface roughness  $R_z$  is the mean of three measurements. According to some previous studies, to achieve the requisite adhesion between the steel substrate and the thermal spray coating, the substrate's surface roughness  $R_z$  should be between 50 and 100  $\mu\text{m}$  [29]-[31].



**Figure 1.** Arc-spray-coated specimens

After finishing sandblasting, the specimens were subjected to the coating process performed on an arc-spray machine (OSU Hessler 300A, Germany) under the conditions recommended by the machine manufacturer, which is as follows:

- Air pressure:  $P = 4.5$  atm.
- Spraying distance:  $L = 300$  mm.
- Spraying angle: 90°.
- Arc potential:  $U = 32$  V.
- Amperage of the current:  $I = 200$  A.

## 2.3. Measurement methods

### 2.3.1. Roughness measurement

The roughness of the sample surfaces was measured by a portable roughness gauge (RUGOSURF 10G, Tesa, Switzerland) with a Gaussian filter, cut-off length  $\lambda_c$  of 0.8 (evaluation length 4 mm). The equipment employs a profile method that utilizes a diamond probe to record surface deviations.

### 2.3.2. Coating adhesion strength measurement

The adhesion strength of the arc-spray coating to the CT3 steel substrate was evaluated using the pull-off technique performed according to JIS H8664-1977 standards on a universal tensile device (AGX-V 50KN, Shimadzu, Japan). The diagram of adhesion measurement is illustrated in Figure 2.

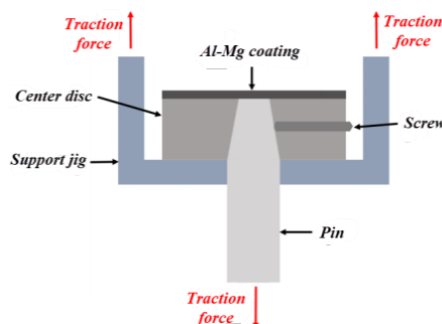


**Figure 2.** Diagram of adhesion measurement

## 3. Results and discussions

### 3.1. Effect of air pressure and spraying distance on surface roughness and coating adhesion strength of CT3 steel specimens

The surface roughness values of steel substrate specimens roughened under the abrasive spraying conditions in Table 3 are listed in Table 4.

**Table 4.** Surface roughness of CT3 steel specimens

Order	$P$ (bar)	$L$ (mm)	Surface roughness $R_z$ ( $\mu\text{m}$ )				Adhesion (MPa)
			Ex 1	Ex 2	Ex 3	Average value	
1	6	100	41.34	41.39	41.35	41.36	9.15
2	6	150	39.16	39.3	39.32	39.26	8.82
3	6	200	37.75	37.6	37.54	37.63	8.53
4	7	100	54.35	54.01	54.3	54.22	12.38
5	7	150	52.4	52.42	51.96	52.26	11.65
6	7	200	50.26	49.87	50.2	50.11	10.72
7	8	100	61.21	61.01	61.32	61.18	14.52
8	8	150	59.35	59.25	59.54	59.38	14.03
9	8	200	55.38	55.49	55.12	55.33	12.85

It is evident from Figure 3 that the surface roughness plays a significant role in determining how well the Al-Mg coating adheres to the substrate. As can be seen, the adhesion strength is almost linearly proportional to the surface roughness within the investigated range. For more information, the surface morphology of the coating on the roughened CT3 substrate is illustrated in Figure 4.

In addition, this investigation intends to determine the extent to which two input parameters of the blasting pressure  $P$  and the blasting distance  $L$  affect the output parameter of surface roughness  $R_z$ . The obtained results

were analyzed using the statistical program Minitab, as shown in Figure 5.

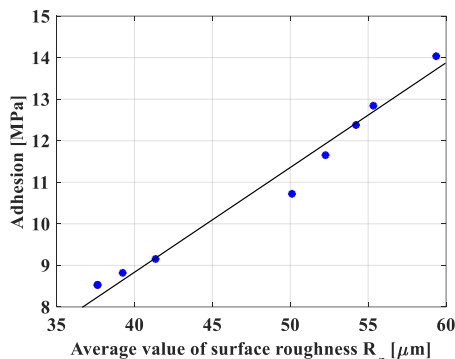


Figure 3. Influence of surface roughness on Al-Mg coating adhesion strength of CT3 steel substrate

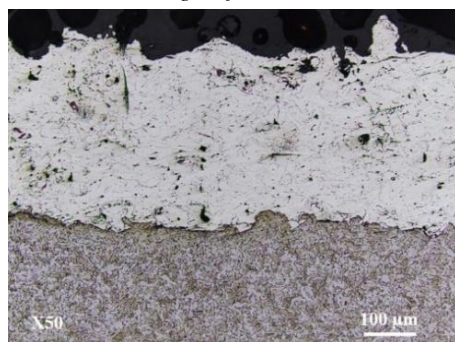


Figure 4. SEM image of Al-Mg alloy coating

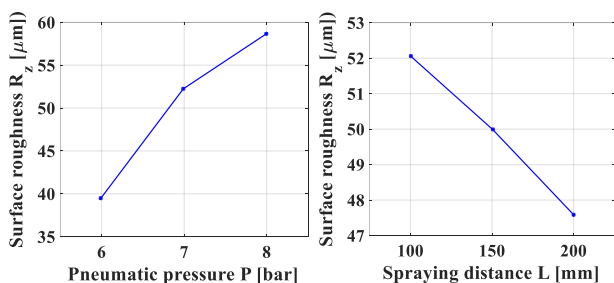


Figure 5. Influence of the input parameters P and L on the surface roughness

Figure 5 illustrates that both input parameters  $P$  and  $L$  have an impact on the output parameter  $R_z$ . When the value of blasting pressure  $P$  is increased, the roughness of surface  $R_z$  tends to rise. In contrast, the roughness of surface  $R_z$  tends to decrease as the stand-off distance  $L$  increases. This is because, as the blasting pressure rises, the abrasive particles are accelerated toward the steel substrate surface, increasing their impact energy. The surface roughness of the steel substrate rises as more metal is expelled from its surface. In contrast, as the stand-off distance between the nozzle and the sample surface increases, the kinetic energy of the abrasive particles decreases, as does the roughening efficiency, leading to low surface roughness [26].

The results of  $S/N$  calculation and analysis from Minitab 16 software are shown in Table 7 and the influence of parameters according to  $S/N$  is shown in Figure 6.

According to Table 7 and Figure 6, we can see that the parameter for the air pressure, which is denoted by  $P$ , has

a greater impact on the surface roughness, which is denoted by  $R_z$ , than the parameter for the spraying distance, which is denoted by  $L$ . When  $P$  is equal to 8 bar and  $L$  is 100 mm, the value of the ratio  $S/N$  is at its highest.

Table 7.  $S/N$  calculation results

Level	$P$	$L$
1	31,91	34,25
2	34,35	33,91
3	35,35	33,46
Delta	3,45	0,79
Rank	1	2

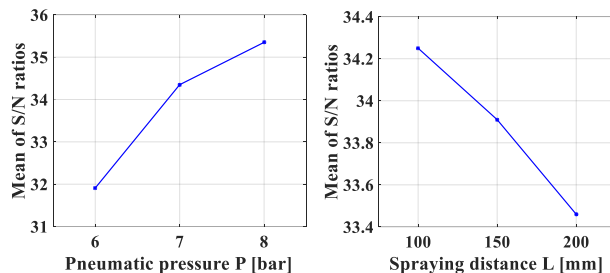


Figure 6. Effect of two input parameters P and L on the S/N ratio

The Analysis of Variance (ANOVA) approach is a tried-and-true technique that is used in conjunction with the "Taguchi" technique to confirm the percentage contribution of each process parameter to the intended outputs. Table 8 illustrates the results of the ANOVA analysis.

Table 8. ANOVA analysis for surface roughness  $R_z$

Source	DF	Seq SS	Adj SS	Adj MS	F	P
P	2	573.868	573.868	286.934	588.97	0.000
L	2	31.452	31.452	15.726	32.28	0.003
Residual error	4	1.949	1.949	0.487	-	-
Total	8	607.269	-	-	-	-

The effect of each input parameter on the output parameter is calculated according to the following equation:

$$\% \text{ influence} = \frac{\text{Seq SS}}{\text{Total}} \times 100\% \quad (2)$$

Figure 8 shows the results of equation (2). As a result, parameter  $P$  has a greater influence on  $R_z$  - about 94.50% - than parameter  $L$ , which has a smaller impact - about 5.18%.

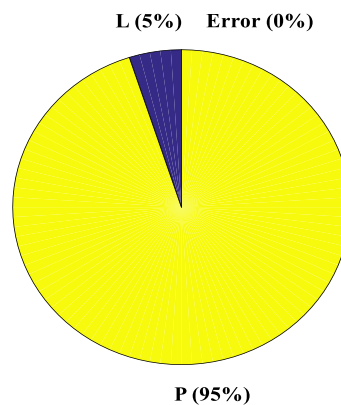


Figure 7. The impact of each input parameter on  $R_z$

### 3.2. Developing regression equations and optimizing the indicators

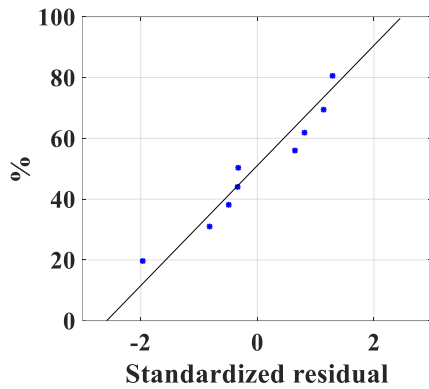


Figure 8. Normal probability of residual, response in means

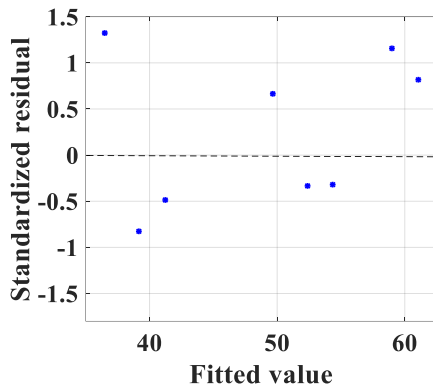


Figure 9. The value distribution of the residual relative to the expected value

The residuals of the regression model are shown in Figure 8 and Figure 9. They are presented to determine whether the regression model meets the assumptions of the analysis. The residual is the deviation of the observed data values from the predicted and estimated errors in the model. The errors are assumed to be random and normally distributed with a mean of zero and a constant standard deviation. Figure 8 shows that the residuals are all close to the diagonal. This proves that the research data set is good and that the normalized residuals have a distribution close to the normal distribution. While Figure 9 shows normally distributed data, outliers do not exist in the data.

If the assumptions are valid, then on the graph of the distribution of the residual relative to the expected value. The residuals and randomly distributed expected values demonstrate the completeness of the model. Figure 9 shows that the normalized residuals do not change in any order concerning the expected value. Therefore, the assumption of a linear relationship is not violated.

Figure 10 is a 3D surface plot used to examine the change of the output parameter for the two expected parameters. The  $R_z$  roughness value is greatest ( $>60 \mu\text{m}$ , yellow region) when the air pressure  $P$  is high and the spraying distance  $L$  is short. The absence of curved lines in the histogram indicates that there is no interaction between the factors.

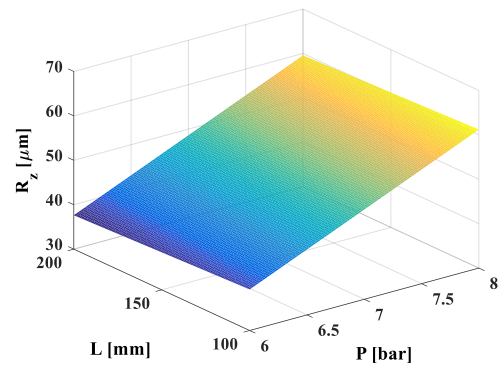


Figure 10. Dependence on surface roughness on two input parameters  $P$  and  $L$

One employs the standard least squares technique to obtain the regression equation in Minitab 16 by minimizing the sum of squared residuals. This research included two active variables with three value levels each. The complete surface roughness regression equation is as follows:

$$y = \beta_0 + \beta_1 x_1 + \beta_2 x_2 \quad (3)$$

where  $y$  is the surface roughness  $R_z$ ;  $\beta_0$ ,  $\beta_1$ , and  $\beta_2$  are coefficients of the regression equation;  $x_1$  and  $x_2$  are the coded coefficients for the air pressure and the spraying distance, respectively. The values of the coefficients of the regression equation for the surface roughness criterion  $R_z$  are presented in Table 9.

Table 9. Coefficients of the regression equation

Term	Coef SE	Coef	T-value	P-value	VIF
Constant	-10.32	6.03	-1.71	0.138	-
$P$	9.607	0.787	12.20	0.000	1.00
$L$	-0.0456	0.0157	-2.90	0.027	1.00

From the data in Table 9, we have developed a first-order regression model showing the relationship between the output parameter  $R_z$  with the input parameters of blasting pressure  $P$  and the stand-off distance  $L$  shown in the following equation:

$$R_z = -10.32 + 9.607P - 0.0456L \quad (4)$$

Table 10. R-value of the regression equation

$S$	$R\text{-sq}$	$R\text{-sq}(adj)$	$R\text{-sq}(pred)$
1.92806	96.33%	95.10%	91.90%

On the other hand, the  $R^2$  value of the regression equation of surface roughness  $R_z$  is 96.33% (Table 10). The  $R^2$ -value is used to evaluate the goodness of fit of the regression model. This shows that the mathematical regression model presented above is the most suitable regression model with two input parameters (the blasting pressure and the stand-off distance) and the output parameter (surface roughness).

By analyzing the results in the optimization function in Minitab 16 software, optimal values of input parameters as well as predicted values of output parameters are obtained. The results are presented in Figure 11 and Table 11.

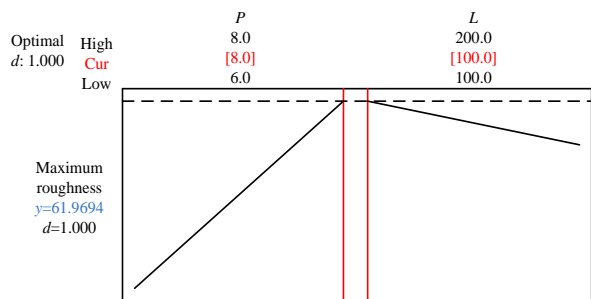


Figure 11. Optimization of air pressure  $P$  and spraying distance  $L$

Table 11. Optimal results of the evaluation criteria.

Air pressure $P$ (bar)	Spraying distance $L$ (mm)	Surface roughness $R_z$ ( $\mu\text{m}$ )
8	100	61,97

Carrying out a verification test of 5 experiments with rough machining parameters as illustrated in Table 11, Table 12 is the test result.

Table 12. Surface roughness of control experiments

Experiments	Surface roughness $R_z$ ( $\mu\text{m}$ )
1	60.25
2	61.19
3	62.36
4	60.04
5	61.66
Average	<b>61.10</b>

Thus, the experiment results show that the average surface roughness  $R_z$  is 61.10 which is close to the optimal value when calculated in Table 12 (61.97). The optimal value of the input parameters as well as the objective function value achieved is to ensure reliability.

In addition, the roughness of surface  $R_z$  in the range of 50-100  $\mu\text{m}$  is satisfactory for the quality of the substrate metal surface treatment for thermal spray coatings, which is covered by three international standards relating to thermal spray. Therefore, the surface roughness  $R_z$  measured in the above optimal technology mode also satisfied the requirements for the quality of the substrate metal surface for the thermal spray coating.

Finally, based on the obtained results, the optimal surface treatment for CT3 steel is given in Table 13.

Table 13. Abrasive spray mode to roughen CT3 steel surface

Order	Mode	Parameter
1	Type of abrasive	Corindon $\text{Al}_2\text{O}_3$
2	Abrasive grain size	#18
3	Air pressure(bar)	8
4	Spraying distance (mm)	100
5	Spraying angle ( $^\circ$ )	90

#### 4. Conclusion

This work researched the influence of the blasting pressure and the stand-off distance on the surface roughness of CT3 steel. Using the Taguchi experimental planning approach and the Minitab 16 statistical software in conjunction with experimentation, this research achieved the following key outcomes:

- It was found that there is a linear relationship between the surface roughness of a CT3 steel and the adhesion strength of an Al-Mg arc spray coating. This relationship shows that adhesion rises as roughness does. At the greatest roughness of 62.17  $\mu\text{m}$ , the highest adhesion value is 14.62 MPa.

- The blasting pressure and the stand-off distance strongly influence the surface roughness of the Rz steel substrate. When the air pressure increases, the surface roughness  $R_z$  tends to increase. Meanwhile, the roughness of surface  $R_z$  tends to decrease with increasing spraying distance. The air pressure has a greater influence than the spraying distance on the surface roughness  $R_z$ . An air pressure of 8 bars and a spray distance of 100 mm were discovered to be the ideal process variables for the greatest surface roughness Rz.

- The mathematical equation showing the relationship between surface roughness  $R_z$  with parameters of blasting pressure and the stand-off distance is developed  $R_z = -10.32 + 9.607P - 0.0456L$ , with a confidence level of 96.33%.

**Acknowledgments:** This work was supported by the key science and technology project of the Vietnam Academy of Science and Technology (Grant TĐVLTT.05/21-23).

#### REFERENCES

- [1] B. Hou, "The cost of corrosion in China", *Cost Corros. China*, pp. 1-941, 2019, doi: 10.1007/978-981-32-9354-0.
- [2] F. Deng, Y. Huang, F. Azarmi, and Y. Wang, "Pitted Corrosion Detection of Thermal Sprayed Metallic Coatings Using Fiber Bragg Grating Sensors", *Coatings*, vol. 7, no. 3, p. 35, 2017, doi: 10.3390/coatings7030035.
- [3] P. A. Sørensen, S. Kiil, K. Dam-Johansen, and C. E. Weinell, "Anticorrosive coatings: A review", *J. Coatings Technol. Res.*, vol. 6, no. 2, pp. 135-176, 2009, doi: 10.1007/s11998-008-9144-2.
- [4] A. Gulec, O. Cevher, A. Turk, F. Ustel, and F. Yilmaz, "Accelerated corrosion behaviors of Zn, Al and Zn/15Al coatings on a steel surface", *Mater. Tehnol.*, vol. 45, no. 5, pp. 477-482, 2011.
- [5] G. Kong and R. White, "Toward cleaner production of hot dip galvanizing industry in China", *J. Clean. Prod.*, vol. 18, no. 10-11, pp. 1092-1099, 2010, doi: 10.1016/j.jclepro.2010.03.006.
- [6] B. Syrek-Gerstenkorn, S. Paul, and A. J. Davenport, "Use of thermally sprayed aluminium (TSA) coatings to protect offshore structures in submerged and splash zones", *Surf. Coatings Technol.*, vol. 374, pp. 124-133, 2019, doi: 10.1016/j.surfcoat.2019.04.048.
- [7] Y. Li, "Corrosion behaviour of hot dip zinc and zinc-aluminium coatings on steel in seawater", *Bull. Mater. Sci.*, vol. 24, no. 4, pp. 355-360, 2001, doi: 10.1007/BF02708631.
- [8] E. Abedi Esfahani, H. Salimijazi, M. A. Golozar, J. Mostaghimi, and L. Pershin, "Study of corrosion behavior of Arc sprayed aluminum coating on mild steel", *J. Therm. Spray Technol.*, vol. 21, no. 6, pp. 1195-1202, 2012, doi: 10.1007/s11666-012-9810-x.
- [9] W. Gu *et al.*, "Deposition of duplex Al<sub>2</sub>O<sub>3</sub>/aluminum coatings on steel using a combined technique of arc spraying and plasma electrolytic oxidation", *Appl. Surf. Sci.*, vol. 252, no. 8, pp. 2927-2932, 2006, doi: 10.1016/j.apsusc.2005.04.036.
- [10] E. Irissou and B. Arsenault, "Corrosion Study of Cold Sprayed Aluminum Coatings onto Al 7075 Alloy", *Therm. Spray 2007 Proc. from Int. Therm. Spray Conf.*, vol. 83676, pp. 549-554, 2007, doi: 10.31399/asm.cp.itsc2007p0549.
- [11] R. M. H. Pombo Rodriguez, R. S. C. Paredes, S. H. Wido, and A. Calixto, "Comparison of aluminum coatings deposited by flame spray and by electric arc spray", *Surf. Coatings Technol.*, vol. 202, no. 1, pp. 172-179, 2007, doi: 10.1016/j.surfcoat.2007.05.067.

- [12] H. Q. Yang, Z. J. Yao, D. B. Wei, W. B. Zhou, G. X. Yin, and L. X. Feng, "Anticorrosion of thermal sprayed Al-Zn-Si coating in simulated marine environments", *Surf. Eng.*, vol. 30, no. 11, pp. 801–805, 2014, doi: 10.1179/1743294414Y.0000000315.
- [13] K. R. Baldwin, R. I. Bates, R. D. Arnell, and C. J. E. Smith, "Aluminium-magnesium alloys as corrosion resistant coatings for steel", *Corros. Sci.*, vol. 38, no. 1, pp. 155–170, 1996, doi: 10.1016/0010-938X(96)00123-0.
- [14] E. Romhanji and M. Popović, "Problems and prospect of Al-Mg alloys application in marine constructions", *Metallurgija*, vol. 12, no. 4, pp. 297–307, 2006.
- [15] Y. Takatani, R. Shindo, K. Togoe, M. Shimatani, and Y. Harada, "Effects of Magnesium Contents in Thermal Sprayed Al-Mg Alloy Coatings on the Corrosion Characteristics", *J. Japan Therm. Spray Soc.*, vol. 51, no. 3, pp. 82–87, 2014.
- [16] R. S. C. Paredes, S. C. Amico, and A. S. C. M. d'Oliveira, "The effect of roughness and pre-heating of the substrate on the morphology of aluminium coatings deposited by thermal spraying", *Surf. Coatings Technol.*, vol. 200, no. 9, pp. 3049–3055, 2006, doi: 10.1016/j.surfcoat.2005.02.200.
- [17] S. Singh, P. Singh, H. Singh, and R. K. Buddu, "Characterization and comparison of copper coatings developed by low pressure cold spraying and laser cladding techniques", *Mater. Today Proc.*, vol. 18, pp. 830–840, 2019, doi: 10.1016/j.matpr.2019.06.509.
- [18] T. Hussain, D. G. McCartney, P. H. Shipway, and D. Zhang, "Bonding mechanisms in cold spraying: The contributions of metallurgical and mechanical components", *J. Therm. Spray Technol.*, vol. 18, no. 3, pp. 364–379, 2009, doi: 10.1007/s11666-009-9298-1.
- [19] S. Singh, H. Singh, S. Chaudhary, and R. K. Buddu, "Effect of substrate surface roughness on properties of cold-sprayed copper coatings on SS316L steel", *Surf. Coatings Technol.*, vol. 389, 2020, doi: 10.1016/j.surfcoat.2020.125619.
- [20] Y. Y. Wang, C. J. Li, and A. Ohmori, "Influence of substrate roughness on the bonding mechanisms of high velocity oxy-fuel sprayed coatings", *Thin Solid Films*, vol. 485, no. 1–2, pp. 141–147, 2005, doi: 10.1016/j.tsf.2005.03.024.
- [21] O. Sarikaya, "Effect of some parameters on microstructure and hardness of alumina coatings prepared by the air plasma spraying process", *Surf. Coatings Technol.*, vol. 190, no. 2–3, pp. 388–393, 2005, doi: 10.1016/j.surfcoat.2004.02.007.
- [22] K. Poorna Chander, M. Vashista, K. Sabiruddin, S. Paul, and P. P. Bandyopadhyay, "Effects of grit blasting on surface properties of steel substrates", *Mater. Des.*, vol. 30, no. 8, pp. 2895–2902, 2009, doi: 10.1016/j.matdes.2009.01.014.
- [23] A. Kemény, I. Hajdu, D. Károly, and D. Pammer, "Osseointegration specified grit blasting parameters", *Mater. Today Proc.*, vol. 5, no. 13, pp. 26622–26627, 2018, doi: 10.1016/j.matpr.2018.08.126.
- [24] M. Mellali, A. Grimaud, A. C. Leger, P. Fauchais, and J. Lu, "Alumina grit blasting parameters for surface preparation in the plasma spraying operation", *J. Therm. Spray Technol.*, vol. 6, no. 2, pp. 217–227, 1997, doi: 10.1007/s11666-997-0016-6.
- [25] M. F. Bahbou, P. Nylén, and J. Wigren, "Effect of grit blasting and spraying angle on the adhesion strength of a plasma-sprayed coating", *J. Therm. Spray Technol.*, vol. 13, no. 4, pp. 508–514, 2004, doi: 10.1361/10599630421406.
- [26] P. Van Lieu, L. T. Quy, and L. T. P. Thanh, "Influence research of surface roughness of the C45 and CT3 steel to quantity of aluminum (Al) coating by thermal spray method", *Vietnam Journals Online*, vol. 50, 2019, [Online]. Available: <https://vjol.info.vn/index.php/dhcnhn/article/view/39727>.
- [27] L. Pawlowski, *The Science and Engineering of Thermal Spray Coatings: Second Edition*, 2008.
- [28] J. J. Pignatiello, "An overview of the strategy and tactics of taguchi", *IIE Trans. Institute Ind. Eng.*, vol. 20, no. 3, pp. 247–254, 1988, doi: 10.1080/07408178808966177.
- [29] ISO 12679:2011, *Thermal spraying – Recommendations for thermal spraying*, International Organization for Standardization, 2011.
- [30] Moduk - DEF STAN 02-828, *Requirements for Thermal Spray Deposition of Metals and Ceramics for Engineering Purposes*, British Defense Standards, 2013.
- [31] NORSOK STANDARD M-501, *Surface preparation and protective coating*, Standards Norway, 2012.